SUPPORTING INFORMATION

Very low frequency broadband EPR spectroscopy of metalloproteins

Wilfred R. Hagen

Department of Biotechnology, Delft University of Technology,
Van der Maasweg 9, 2629HZ Delft, The Netherlands
w.r.hagen@tudelft.nl

A – Spectrometer hardware (detailed parts list)
B- Additional cytochrome EPR data
C- Software (programs to simulate inhomogeneous broadened spectra)

Part-A – Spectrometer hardware (Figures S 1 - S 3, Tables S 1, S 2)

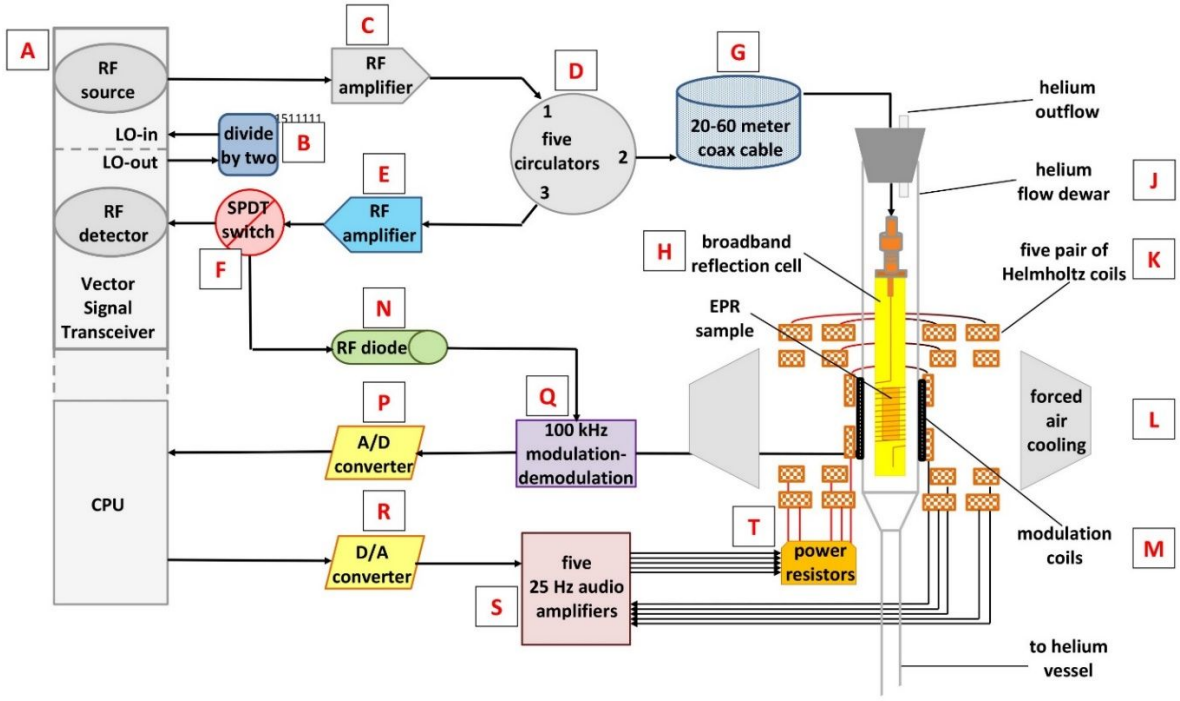

Figure 1. Detailed description of the broadband spectrometer. A complete list of individual components follows (Table S 1). The depicted magnet configuration is for low microwave frequency operation (65 to circa 700 MHz). Adjustments required for higher frequencies up to 18 GHz are given in a subsequent list (Table S 2)

Table S 1. List of individual spectrometer parts.

[A] A Vector Signal Transceiver NI PXIe-6644R (0.065-6.000 GHz source and detector) and a NI PXIe-8135 embedded controller (CPU) in a NI PXIe-1075 chassis (National Instruments, Austin, TX).

[B] Active divider-by-two FPS-2-20 (RF Bay, Gaithersburg, MD); the output is reduced by a 6 dB line attenuator so that overall loss is 0 dB. The divider is engaged for frequencies < 375 MHz to comply with the local oscillator output of the RF detector.

[C] RF amplifier NI PXI-5691 (0-8 GHz) build in the PXIe-1075 chassis.

[D] (i) Broadband circulator UIYBCC6060A (68-88 MHz) (UIY, Shenzhen, China).
(ii) Broadband circulator VAB1496 (100-200 MHz) (Valvo Bauelemente, Hamburg, Germany)
(iii) Broadband circulator UIYBCC5377A (225-400 MHz) (UIY, Shenzhen, China)
(iv) Circulator UIYCC4550A450T600SF (450-600 MHz) (UIY, Shenzhen, China)
(v) Circulator JXWBHX-T-820-880-20 (740-830 MHz) (A-INFO, Irvine, CA). This component was obtained second-hand (via eBay) and was found to operate over the 630-780 MHz range.

[E] Unbranded 4W RF amplifier (10-1000 MHz) (via eBay, China).

[F] RF switch NI PXI-2599 (National Instruments)

[G] Up to three unbranded coils (16 cm outer diameter) of 20 meter length RF coaxial RG402 cable (via eBay, China).

[H] The broadband wire micro strip reflection cell has been described in detail in (1). In the present work the copper base plate has been replaced with aluminium and the lacquered copper micro wire has been replaced with a bare silver micro wire for work on (frozen) solutions of chemicals showing reactivity with copper.

[J] This simple glass dewar was designed by S. Albracht for the Varian E-line Q-band spectrometer (4).

[K] The outer two pairs of coils are U8481500 (3B Scientific, Hamburg, Germany); they have a diameter of d = 300 mm and a total resistance R = 2.3 Ω. Then there are two pairs of homemade coils, the outer one wound to d = 250 mm from 1.18 mm enamelled copper wire, and the inner one wound to d = 225 mm from 1.12 mm wire. Pair resistances are circa 2 Ω. The fifth coil pair was taken from the rapid-scan unit of a Bruker ER 200D spectrometer. It has d = 104 mm from 0.4 mm enamelled copper wire {book-7 page 23} and R = 4.4 Ω. The gap between these coils is 52 mm. The

coils are fixed in a wooden frame on top of a stainless-steel frame of dimensions such that a 50 L liquid helium vessel can be placed underneath the coils for insertion of the flow dewar.

[L] Two 62 W centrifugal ventilators (d = 125 mm) for household use (Maxeda, Amsterdam, Netherlands) were purchased from a local do-it-yourself shop. Each ventilator has a volumetric flow rate of 388 m^3/h adding up to a total of 216 L/s. With d = 125 mm flexible tubing the air is led to outlets fixed close to the exterior of the Helmholtz coils.

[M] These coils were taken from a Varian E-line Q-band spectrometer, and were designed to be operated with the E-line modulation unit (see under [Q]). They are rectangular (side = 40 mm) and folded around a cylinder of inner d = 40 mm.

[N] Zero-bias Schottky RF diode CPDETLS-4000 (10-4000 MHz) (Crystek Corporation, Fort Myers, FL), or PE8013 (10-18500 MHz) (Pasternack Enterprices Inc., Irvine, CA).

[P] Data acquisition device NI USB-6351 (National Instruments).

[Q] Modulation-demodulation unit (100 kHz) taken as two units ('system function selector' and '100 kHz') form the console of a Varian E-line spectrometer and re-wired to a ± 20 V external power supply.

[R] Data acquisition device NI USB-6001 (National Instruments).

[S] (i) Audio stereo amplifier Crown XTi 6002 producing 6000 W at 4 Ω impedance in bridged mode (Harman International, Elkhart, IN).
(ii) Three pieces of audio stereo amplifier Europower EP 4000 each producing 4000 W at 4 Ω impedance in bridged mode (Behringer, Willich, Germany).
(iii) Audio stereo amplifier t.amp E-800 producing 1000 W at 4 Ω impedance in bridged mode (Musikhaus Thoman, Burgebrach, Germany).

[T] Power resistors type RB101 (100 W, 1 Ω) (ATE Electronics, Giaveno, Italy) were used to increase the total resistance of each coil-pair circuit to match, or exceed, the 4 Ω impedance of the audio amplifiers. The resistors were attached with Al_2O_3 paste to an aluminum heat sink which was air-cooled by five F8 case fans with fluid dynamic bearing (Arctic, Braunschweig, Germany).

Table S 2. Modifications for higher frequencies (ca 500-18000 MHz) and slow field scan.

[I] To up-convert the primary frequency of the RF source into the 6-18 GHz range a varying combination of two doublers is used. The active doublers are the MAX2M060260 with 3-13 GHz input and the MAX2M080160 with 4-8 GHz input (Narda-Miteq, Hauppauge, NY).

[II] The signal out of port 3 of the circulator is now amplified with a DB98 (600-8000 MHz) (Narda-Miteq, Hauppauge, NY) or with a GNA-157F (6-18 GHz) (RF Bay, Gaithersburg, MD).

[III] The power out of the amplifier under [II] as a function of frequency is measured with an NI USB-5681 power meter (10-18000 MHz) (National Instruments).

[VI] The very long (20-60 m) coaxial elongation cable is replaced with a shorter one typically some 2 m in length.

[V] Following port 2 of the circulator a trombone-type phase shifter is inserted for tuning the dip of the resonator circuit to optimal depth. For up to 4 GHz the make is model D4428C (Arra Inc., Bay Shore, NY); at higher frequencies it is Pasternack Enterprices model PE8255 (Pasternack Enterprices Inc., Irvine, CA).

[VI] Additional circulators are
(i) TMRF 3X15 (1085-1580 MHz) (RYT Industries Inc., Santa Clara, CA).
(ii) Type 300360 (1400-2800 MHz) (RYT Industries Inc., Santa Clara, CA).
(iii) PE8432 (2-6 GHz) Pasternack Enterprices Inc., Irvine, CA).
(Iv) C-8S63T-7C (7-16.2 GHz) (Microwave Associates Inc., Lowell, MA).
(v) Type I4C (10.7-17.9 GHz (unknown brand).

[VII] The multi-coil magnet is replaced with a conventional, water-cooled 2.7 kW electromagnet B-MN 90V/30A (Bruker BioSpin GmbH, Rheinstetten, Germany) driven by a custom-made Magnet Power Supply 858 System 8500, 90V/30A (Danfysik A/S, Taastrup, Denmark).

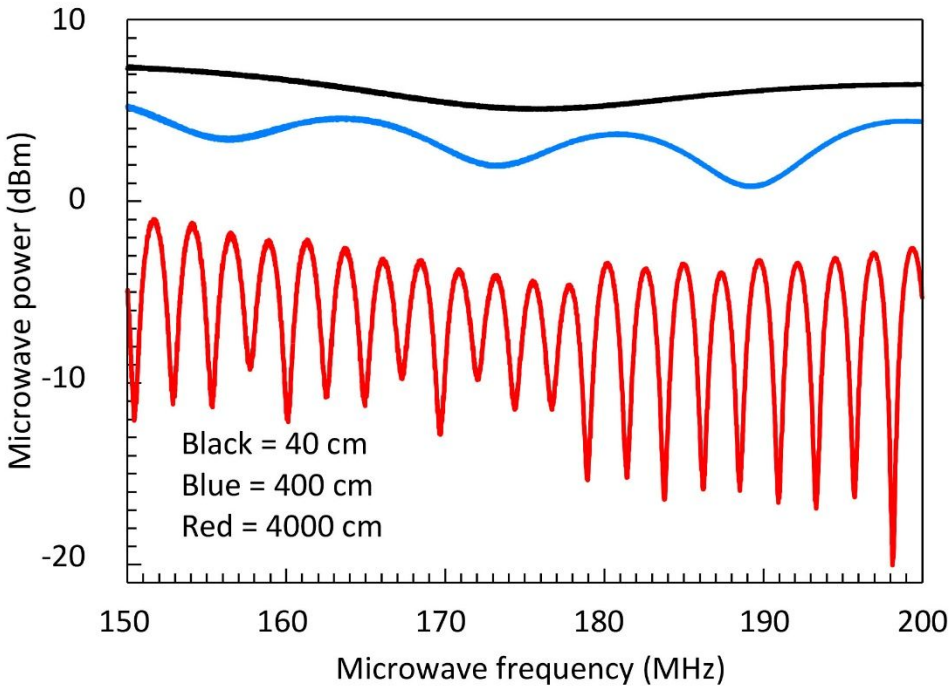

Figure S 2. Reflected mode pattern of the resonator circuit at low microwave frequencies. The circuit is as in Figure 1 or Figure S 1 starting at port 2 of the circulator. The pattern is detected at the monochromatic RF detector of the VST in a frequency scan. The figure illustrates the necessity to use very long coaxial elongation cables to create multiple deep resonance dips.

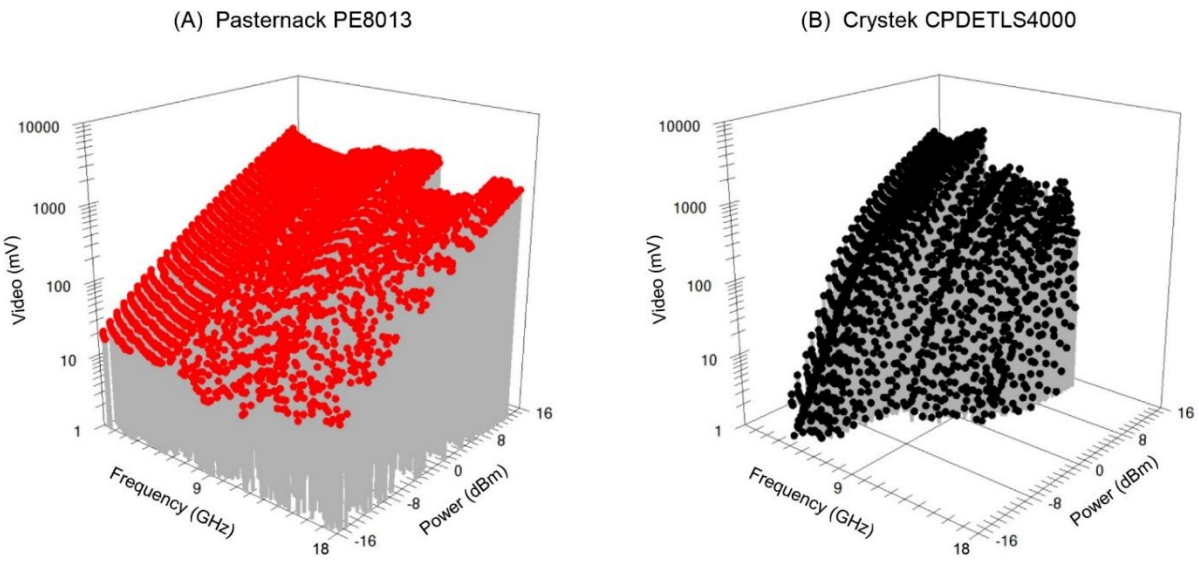

Figure S 3. Transfer function of Schottky-type RF detectors. Broadband EPR can be detected with RF diode assemblies which should be preferably employable over a wide frequency range. Here, two types are used, the Pasternack PE8013 (10-18500 MHz) and the Crystek CPDETLS-4000 (10-4000 MHz). Their transfer function was determined with the VST as microwave source (65-6000 MHz) in combination with two frequency doublers (cf Figure 2). The microwave power output was measured with a National instruments USB-5681 Power Meter (10-18000 MHz) and then switched into the detection diode. The video output of the diode was measured with a National Instruments USB-4065 digital multimeter device. In panel (A) the PE8013 is seen to respond linearly with a strong video signal over the entire frequency range and over a power range of -16 to circa +14 dBm. The response of the Crystek CPDETLS4000 (panel B) deteriorates above 4 GHz and its video signal is linear only above some 0 dBm input power. However, it has the advantage to accept higher powers up to +30 dBm, where the PE8013 is limited to +20 dBm. It is also an order of magnitude cheaper.

Part B – Additional cytochrome EPR data (Figures S 4 - S 13)

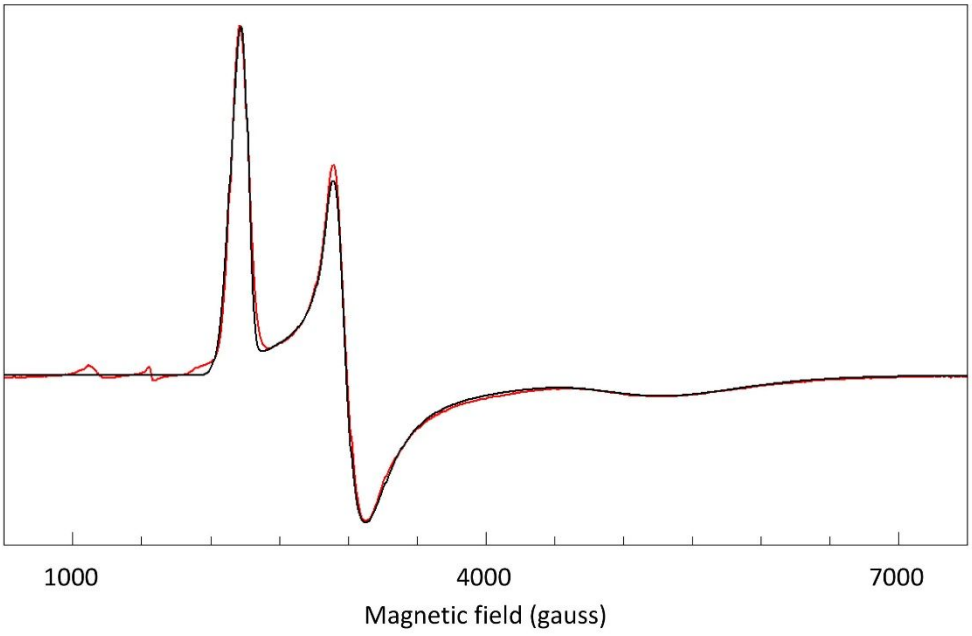

Figure S 4. g-Strain simulation of the X-band EPR spectrum of cytochrome c. The sample was 5.5 mM horse heart cytochrome c (Sigma-Aldrich C2506) in 100 mM potassium phosphate buffer, pH 7.4. This simulation has been carried out before (5), however, since then the formal definition and physical interpretation of g strain has been modified (43,44), therefore the exercise is repeated here. Simulation parameters using the program GeeStrain-5: $g_{x,y,z}$= 1.20, 2.228, 3.056; $\Delta g_{xx,yy,zz}$=0.13, 0.09, -0.10; $\Delta g_{xy,xz,yz}$=0.05, 0.06, 0.13; $\Delta g_{residual}$=0.05; steps in $\cos\theta \times \varphi$ over half a unit sphere = 100 × 100. Experimental conditions: microwave frequency, 9407.513 MHz; microwave power, -10 dB of 200 mW; modulation frequency, 100 kHz; modulation amplitude, 10 gauss; temperature, 20 K.

REFRENCES

(43) Hagen, W.R.; Hearshen, D.O.; Sands, R.H.; Dunham, W.R. A statistical theory for powder EPR in distributed systems. *J. Magn. Reson.* **1985**, 61, 220-232.

(44) Hagen, W.R.; Hearshen, D.O.; Harding, L.J.; Dunham, W.R. Quantitative numerical analysis of g strain in the EPR of distributed systems and its importance for multicentre metalloproteins. *J. Magn. Reson.* **1985**, 61, 233-244.

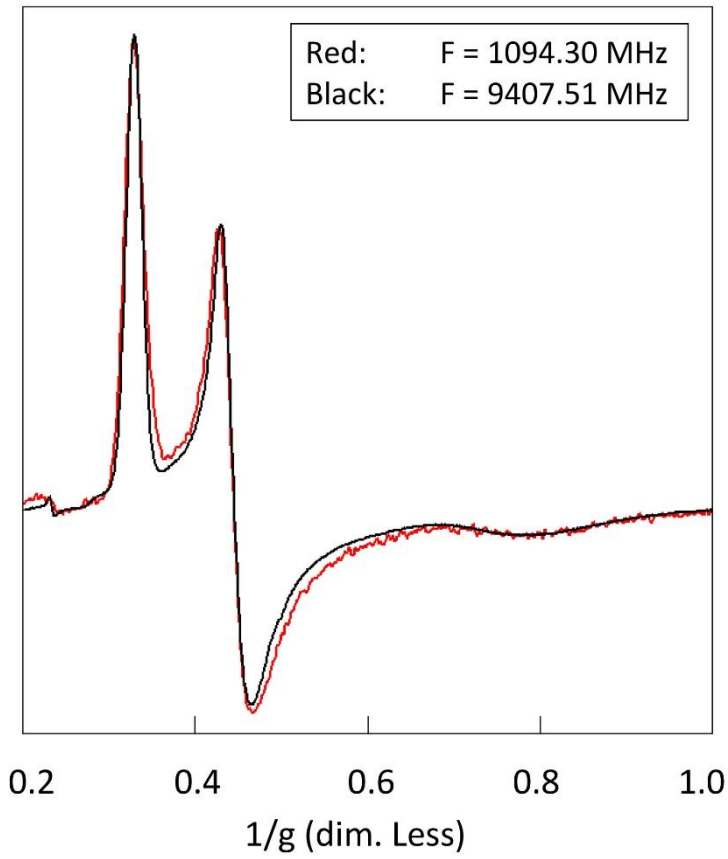

Figure S 5. Comparison of the inhomogeneous broadening of cytochrome c EPR in X-band versus L-band. Overlay of the spectra taken at 9407.51 MHz and 1094.30 MHz on a reciprocal g-value scale shows that broadening is dominated by g strain over the complete spectrum (that is, invariant with frequency) with minor additional broadening especially for intermediate orientations (that is, the magnetic-field vector not along any of the g tensor principal axes). Experimental conditions: X-band as in Figure S 4; L-band, dip power, +11.8 dBm; modulation frequency, 100 kHz; modulation amplitude, 4.9 gauss; temperature, 13 K; 50 scans of 20 s were averaged.

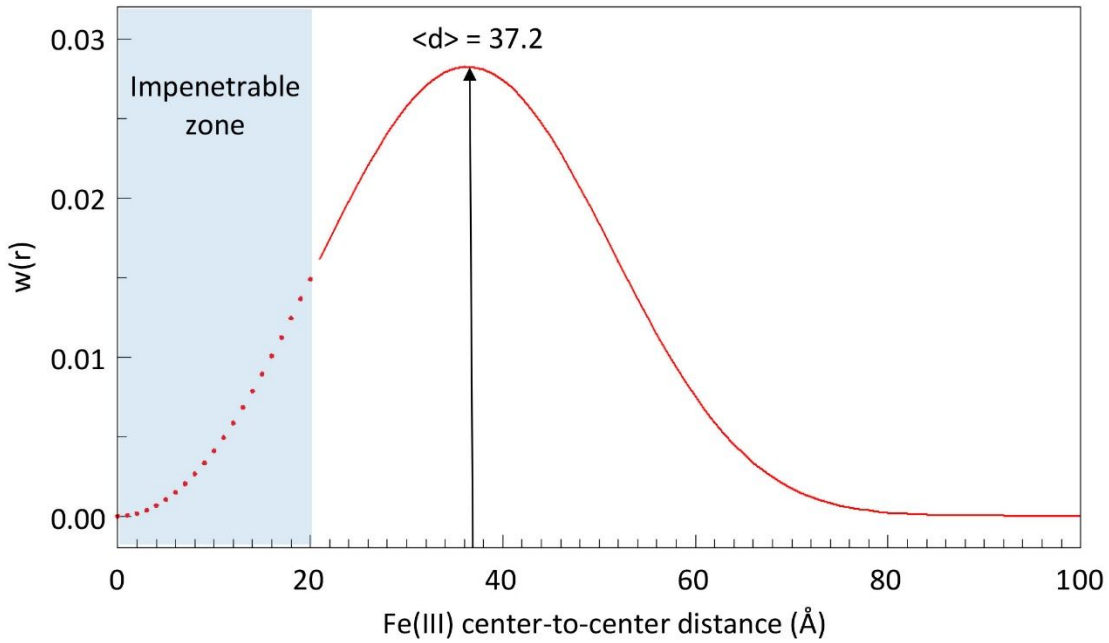

Figure S 6. Distribution of nearest neigbors as a function of distance in a random distribution of particles. The function w(r) is the probability that the nearest neighbor is found at a distance between r and r+1 Å. The discrete integral of the distribution is unity. The particles are taken to be cytochrome c molecules, which are approximated as spheres of circa 20 Å diameter with the iron ion in the center. The impenetrable zone arises because the centers of two cytochrome c 'spheres' cannot approach closer than 20 Å when the outsides of two spheres touch. <d> is the average distance in Å for a given concentration. This stochastic description is due to Chandrasekhar (20).

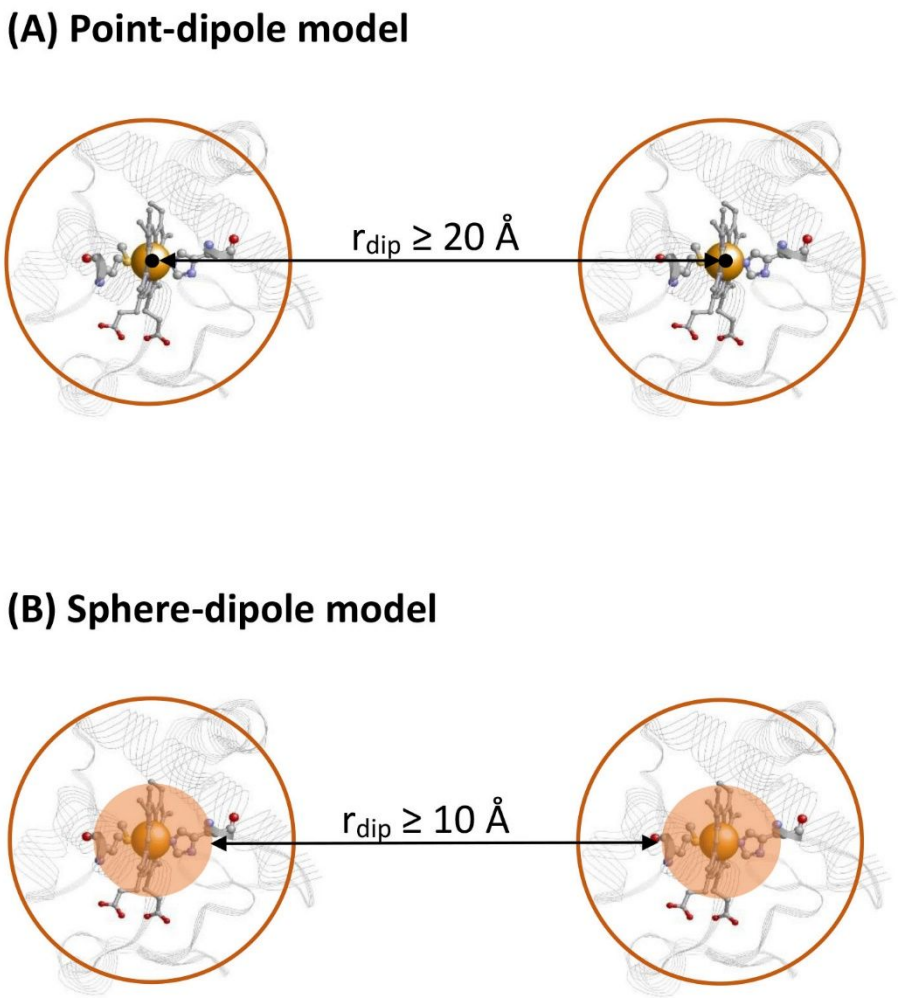

Figure S 7. Two alternative models for intermolecular dipole-dipole interaction between cytochrome c molecules. (A) The classical point dipole model assumes the paramagnetic dipoles to be of infinitesimal size, which implies that their minimal distance is limited only by the size of the protein 'sphere'. (B) In the sphere-dipole model the size of the dipoles is assumed to be finite, and is here approximated as a sphere of radius 5 Å around the Fe(III) ion, which roughly corresponds to a distance from the iron to a point in between the outer tetrapyrrole ring and the alpha carbons of the side chains. Spin density on the protons of the α-CH_2';s have been observed in double-resonance experiments (7,8). The minimum distance between the Fe centers is now the radius of the protein sphere minus the radius of the dipole sphere, that is, 10 Å.

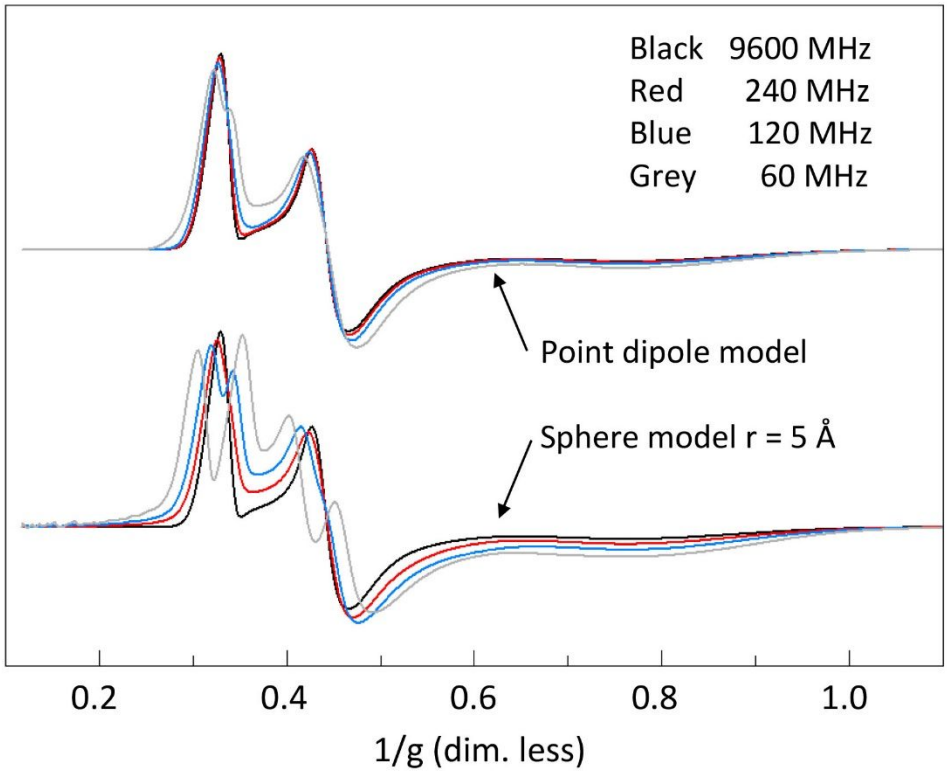

Figure S 8. Simulation of broadening under alternative dipolar models in addition to g strain in the spectrum of cytochrome c. The simulation assumes eight neighbors at the corner of a cube surrounding a central cytochrome c molecule whereby the distance to the corners is stochastically distributed as given in Figure S 6. In the spectral sets for the two models the black trace is the high-frequency limit in which there is only g-strain broadening (cf Figure S 4). Lowering the frequency increases the dipolar contribution as indicated. The simulations are based on 346 equidistant steps in the stochastic distribution in Figure S 6 for a concentration of 5.5 mM and assuming a cutoff of 20 Å. It can be observed that under the point dipole model dipolar broadening starts to significantly contribute only as frequencies well below those used for cytochrome c EPR in Figure 5, while on the other hand under the sphere model significant broadening is expected to appear around some 240 MHz.

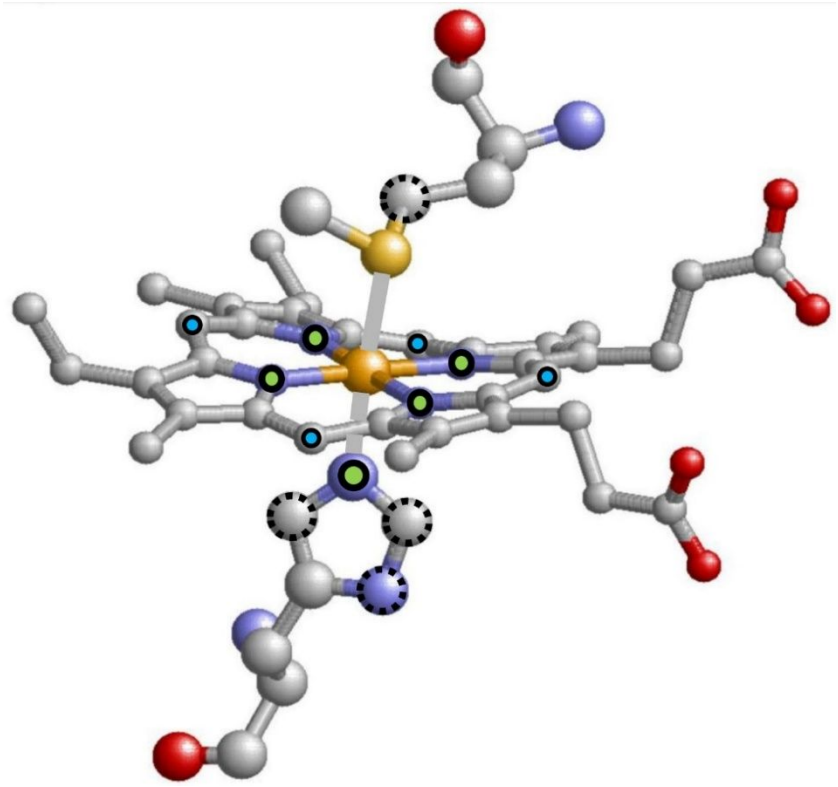

Figure S 9. Outline of nitrogen and hydrogen nuclear spins that have been reported to be magnetically coupled to the electron spin of Fe(III) in hemoproteins. The data are from ENDOR and ESEEM studies on low-spin derivatives of myoglobin (7-9,11-13,17) and on cytochromes a (10), b_{559} (14), and c_6 (15,16), where studies on cytochrome c were inconclusive for unknown reasons (7,9). Reported superhyperfine splittings were typically in the range 1.4-1.6 gauss, with occasional values of 1.9 gauss (7) for the ^{14}N's of the tetrapyrrole system and the coordinating nitrogen of histidine or imidazole axial ligand (black-circled green dots), of the order of 1 gauss for certain protons on histidine, imidazole, and methionine axial ligands (broken black circles), circa 0.25 gauss for the meso-protons of the tetrapyrrole system (black-circled blue dots), and some 0.15 gauss for protons in the side chains of the pyrrole ring system. The latter are not indicated in the figure because different studies give different chemical assignments (e.g., side chain α-CH_2 (7,8) versus pyrrole methyl (15)).

Based on these data I expect for the present study a significant SHF contribution in the low-frequency (232 MHz) CW-EPR of cytochrome c from five ^{14}N, I = 1 spins in the form of broadening, but no resolution, e.g., due to variations in the individual SHF values, due to anisotropy, and due to the blurring effect of the five H, I = 0.5 spins in the axial ligands. Contributions of the other (meso and external) protons is deemed too weak to contribute to the EPR broadening.

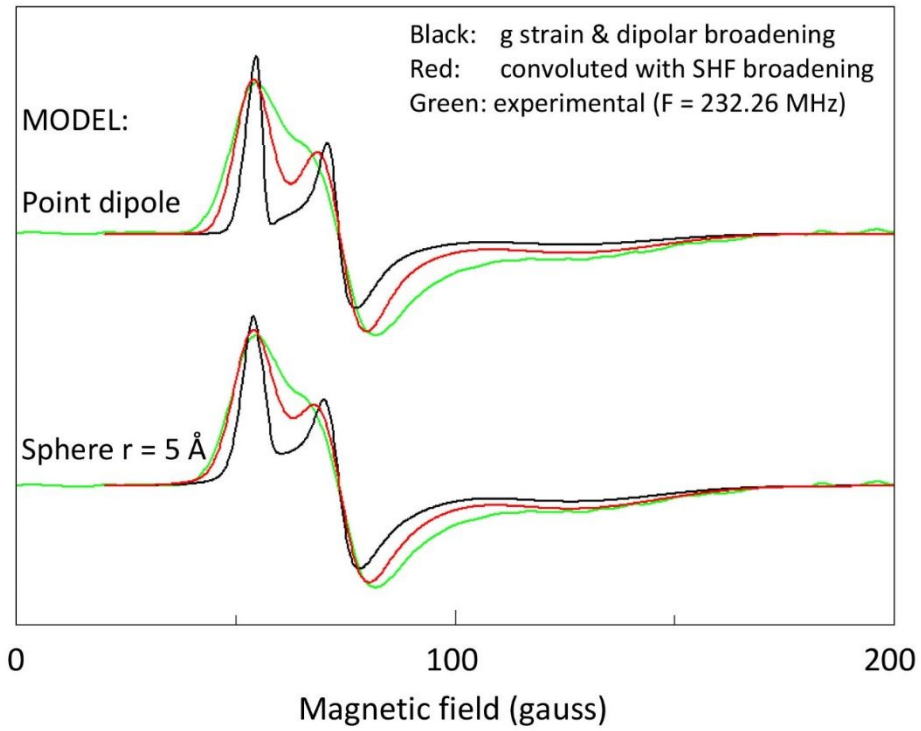

Figure S 10. Simulation of the inhomogeneously broadended 232 MHz spectrum of cytochrome c under two different dipole models. Black traces are simulations assuming g-strain and dipolar broadening as described in Figures S 6 – S 8. A total of 346 equidistant steps were made in the stochastic distribution of Figure S 6 for a concentration of 5.5 mM and assuming a cutoff of 20 Å. The g-strain simulation used the parameters determined in Figure S 4. The red traces are convolutions of the black traces with SHF coupling from five nitrogens with isotropic A_N = 1.7 gauss and five protons with A_H = 1.0 gauss. Under the point-dipole model the convoluted shape falls significantly short of explaining the overall broadening of the experimental spectrum. Under the sphere-dipole model the discrepancy is largely resolved in the g_z and g_x direction with some remaining lack of broadening in the simulation at intermediate orientations. Experimentally, extra broadening for intermediate orientations was also observed in Figure S 5.

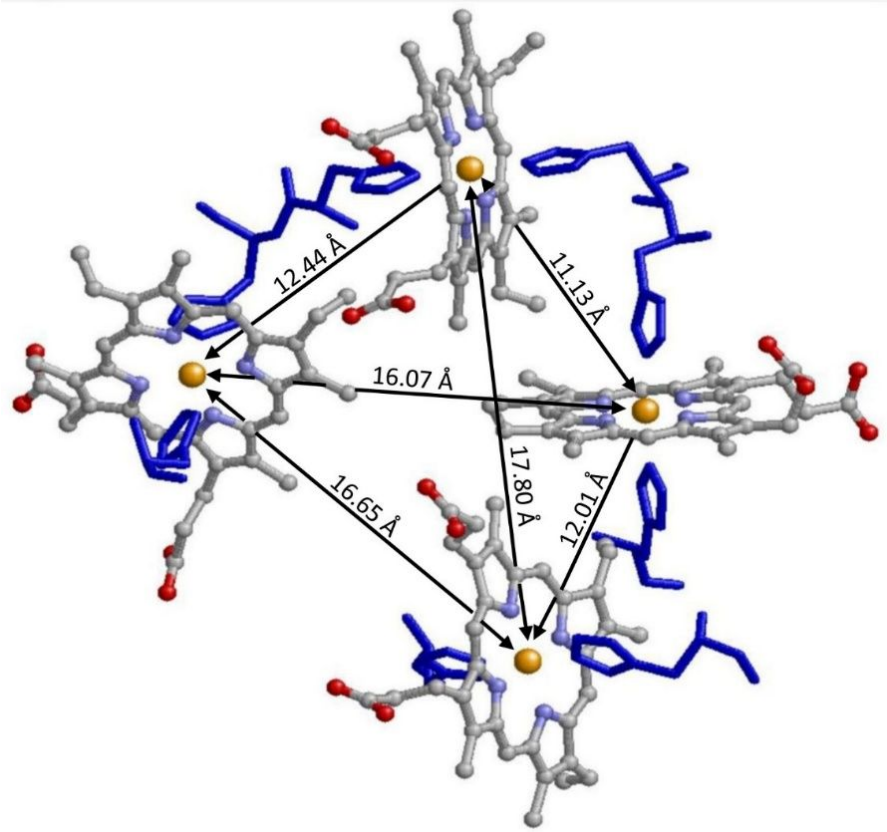

Figure S 11. Iron-to-iron distances for the four hemes in cytochrome c_3. The figure depicts the hemes and the eight histidine axial ligands taken from the crystal structure 2CTH.pdb *of Desulfovibrio vulgaris*, substrain Hildenborough (38). The six metal-to-metal distances can be arranged into two groups: relatively short distances of circa 11-12 Å and longer distances of circa 16-18 Å. This grouping predicts two 'waves' of dipolar broadening of the EPR as function of decreasing microwave frequency.

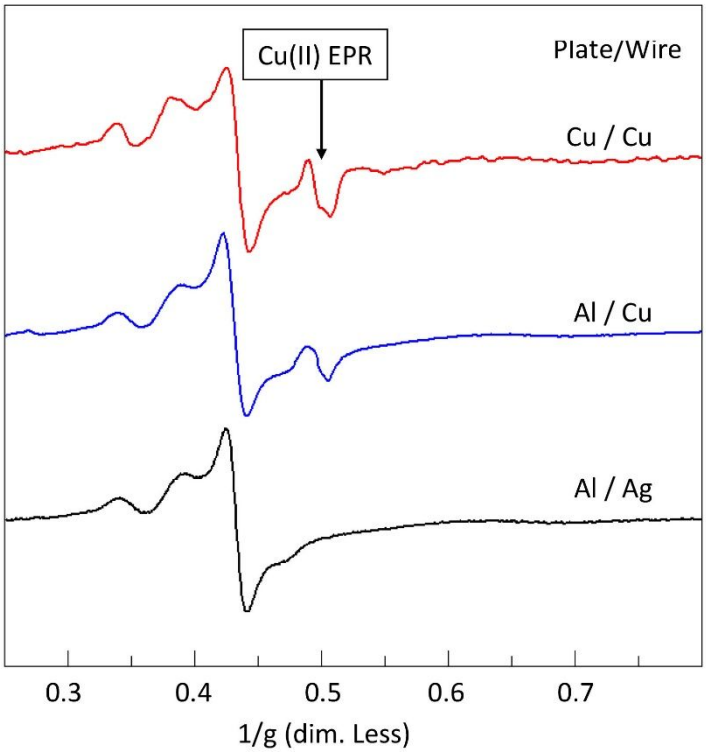

Figure S 12. Contamination of the 2-GHz spectrum of cytochrome c_3 with a signal form copper ions dissolved from the sample cell. The spectra (from top to bottom) were taken at 2112, 1952, and 1942 MHz. The original micro strip broadband sample cell consisted of a bare copper base plate of 1 mm thickness surrounded by diamagnetic acrylic tape of 200 µm thickness, with some tape cut away to provide space for the paramagnetic sample, and with the tape and sample topped by a lacquered copper wire of 200 µm spiralling over the sample (1). For low-temperature measurements of metalloproteins the protein solution would be placed in the sample compartment with direct contact to the bare copper base plate, and the cell plus sample would be frozen by horizontal placement on an aluminium slab previously cooled by prolonged immersion in liquid nitrogen. With this approach I would repeatedly find adventitious copper signals in the spectra of metalloproteins such as in the top trace spectrum of cytochrome c_3. Replacing the copper plate with an aluminium one of identical dimensions did not affect the microwave transmission/reflection properties of the cell; it reduced the adventitious copper signal but did not completely abolish it as illustrated in the middle trace spectrum. Subsequent replacement of the copper wire with bare silver wire again did not affect the RF properties of the cell but the copper signal completely disappeared as shown in the lower trace spectrum. Therefore, in the present study aluminium plate/silver wire cells have been used for metalloprotein EPR.

Part C – Software

All source codes are in file PROGRAMS_CODE.zip

Software was typically written in mixed-language, LabVIEW graphical language, using the LabVIEW professional development system 2020 with calls to dynamic link libraries for the computational-intensive procedures written in FORTRAN using the Intel® Visual Fortran Compiler 2020 integrated into the Microsoft Visual Studio Community 2019 development environment.

The set of programs used to simulate inhomogeneous broadening from a combination of g strain, dipolar interaction, and superhyperfine (SHF) interaction are outlined below. Executables and full source code, including all subroutines and dynamic link libraries, is provided in a separate zip file.

The set of programs to calibrate and run the spectrometer is dedicated to the specific collection of hardware items used in the present study and is therefore not included here. Since parts of the code may be of interest for application in alternative setups, the source code of the complete set is available upon request.

The program GeeStrain5 to simulate the sum-spectrum of up to five independent spectra determined by g strain has previously been described and made available as executable (2). It has been re-checked, rewritten as a DLL and combined with a LabVIEW graphic user interface which can be easily adjusted to personal preferences. The full source code is now also made available.

Analysis of inhomogeneous broadening (here in the low-frequency EPR of cytochrome c) proceeds in three steps:

(1) The program **GeeStrain5** is used to simulate a single high-frequency (that is, X-band) spectrum assuming that the spectrum is determined by g-strain broadening only (cf Figure S 4). Fitting parameters are the 3 g values, the 6 elements (that can be positive or negative) of the g-strain tensor, and a residual broadening to prevent divide-by-zero and to accommodate

any additional broadening. The output spectrum (that is, optimized fitting parameters) is input to the next two programs to calculate g strain by transformation to lower frequency.

(2) The program **GstrainWithDipolar** convolutes g strain with intermolecular dipole-dipole interaction (cf Figure S 8). Concentration of the paramagnet must be entered. Fitting parameters are the radius of the sphere that approximates the globular protein surrounding the paramagnet and the radius of the sphere that approximates the finite geometry of the paramagnetic dipole. The program does full energy-matrix diagonalizations for a paramagnet subject to dipolar interaction with eight copy molecules at the corners of a cube. The result is compared with an experimental spectrum taken at low frequency. The program was used to show that these two broadening mechanisms together were insufficient to explain the overall broadening in the 232 MHz spectrum of cytochrome c.

(3) The program **GstrainWithDipolarAndSHF** takes the output of program-2 and convolutes this with isotropic superhyperfine from nitrogen and hydrogen ligands. The splittings, that is, the fitting parameters, were estimated for cytochrome c from literature on double-resonance experiments of hemoproteins. The result is compared with an experimental spectrum taken at low frequency (cf Figure S 10). Example spectra are included.